Journal of Atmospheric and Solar-Terrestrial Physics 73 (2011) 2331–2344

Contents lists available at ScienceDirect

Journal of Atmospheric and Solar-Terrestrial Physics

journal homepage: www.elsevier.com/locate/jastp

Variation in surface air temperature of China during the 20th century

Willie Soon [a,*], Koushik Dutta [b], David R. Legates [c], Victor Velasco [d], WeiJia Zhang [e]

[a] Harvard-Smithsonian Center for Astrophysics, Cambridge, MA 02138, USA
[b] Large Lakes Observatory, University of Minnesota-Duluth, Duluth, MN 55812, USA
[c] College of Earth, Ocean, and Environment, University of Delaware, Newark, DE 19716, USA
[d] Departamento de Investigaciones Solares y Planetarias, Instituto de Geofisica, Universidad Nacional Autonoma de Mexico, Ciudad Universitaria, C.P. 04510, Mexico
[e] Department of Physics, Peking University, Beijing 100871, China

ARTICLE INFO

Article history:
Received 21 March 2011
Received in revised form
20 July 2011
Accepted 25 July 2011
Available online 3 August 2011

Keywords:
Total solar irradiance
Sunshine duration
Surface air temperature
Circum-global teleconnection

ABSTRACT

The 20th century surface air temperature (SAT) records of China from various sources are analyzed using data which include the recently released Twentieth Century Reanalysis Project dataset. Two key features of the Chinese records are confirmed: (1) significant 1920s and 1940s warming in the temperature records, and (2) evidence for a persistent multidecadal modulation of the Chinese surface temperature records in co-variations with both incoming solar radiation at the top of the atmosphere as well as the modulated solar radiation reaching ground surface. New evidence is presented for this Sun–climate link for the instrumental record from 1880 to 2002. Additionally, two non-local physical aspects of solar radiation-induced modulation of the Chinese SAT record are documented and discussed.

Teleconnections that provide a persistent and systematic modulation of the temperature response of the Tibetan Plateau and/or the tropospheric air column above the Eurasian continent (*e.g.*, 30°N–70°N; 0°–120°E) are described. These teleconnections may originate from the solar irradiance-Arctic–North Atlantic overturning circulation mechanism proposed by Soon (2009). Also considered is the modulation of large-scale land–sea thermal contrasts both in terms of meridional and zonal gradients between the subtropical western Pacific and mid-latitude North Pacific and the continental landmass of China. The Circum-global teleconnection (CGT) pattern of summer circulation of Ding and Wang (2005) provides a physical framework for study of the Sun–climate connection over East Asia. Our results highlight the importance of solar radiation reaching the ground and the concomitant importance of changes in atmospheric transparency or cloudiness or both in motivating a true physical explanation of any Sun–climate connection. We conclude that ground surface solar radiation is an important modulating factor for Chinese SAT changes on multidecadal to centennial timescales. Therefore, a comprehensive view of local and remote factors of climate change in China must take account of this as well as other natural and anthropogenic forcings.

© 2011 Elsevier Ltd. All rights reserved.

1. Introduction

Instrumental temperature records in China for the 20th century have long been suggested to represent variations and changes of climate for an area far broader than China alone (Zhu, 1973; Bradley et al., 1987; Wang and Gong, 2000; Tang et al., 2009). As early as 1962, Chinese surface air temperature (SAT) records constructed by Wang et al. (2001, 2004) were shown to contain significant warming peaks and trends in the first half of the 20th century. The final compilation (summarized in Wang et al. (2001, 2004) with the most recent update and intercomparison reported by Tang et al. (2009)) aggregated from ten regional SAT series from 1880 to 2002 shows three significant decade-long warming intervals during the 1920s, 1940s, and 1990s (see highlights in Fig. 1a) as well as the extended relative cooling phase between the 1950s and early 1980s. The early 20th century warming in China offered the opportunity for a full examination of the concomitant natural warming across the globe with evidence extending across the Arctic–North Atlantic–North American–North Pacific regions (Diaz and Quayle, 1980; Rogers, 1985; Fu et al., 1999; Drinkwater, 2006; Holland et al., 2008; Kauker et al., 2008; Box et al., 2009; Bronninmann, 2009; Helama et al., 2010; Wood and Overland, 2010; Wood et al., 2010; Frauenfeld et al., 2011; see also Soon (2009) for additional evidence and synthesis) to the Indian ocean and tropical Pacific (Fu et al., 1999; Giese et al., 2010). It is important to note that the warming of the 1920s can be shown to relate to warming in the subsurface water in the Greenland and North Atlantic regions (Drinkwater, 2006; Holland et al., 2008).

* Corresponding author.
E-mail address: wsoon@cfa.harvard.edu (W. Soon).

1364-6826/$ - see front matter © 2011 Elsevier Ltd. All rights reserved.
doi:10.1016/j.jastp.2011.07.007

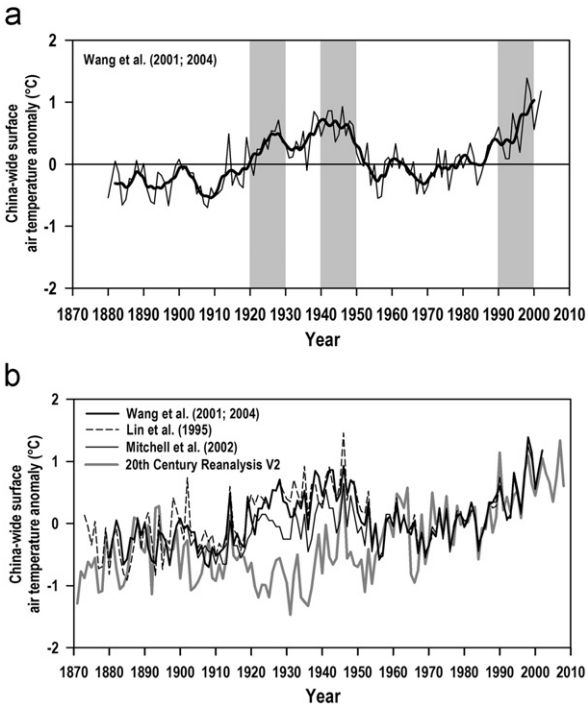

Fig. 1. (a) The Chinese temperature record of Wang et al. (2001, 2004) adopted in this study highlighting the 3 decade-long warm intervals of 1920s, 1940s and 1990s. (b) China-wide surface air temperature series from 1870 to 2008 based on the construction by: (1) Peking University (Wang et al., 2001, 2004), (2) the Chinese Academy of Meteorological Science (Lin et al., 1995), (3) the University of East Anglia's Climatic Research Unit (Mitchell et al., 2002), and (4) the 20th Century Reanalysis Project V2 (20CRv2) dataset (Compo et al., 2011).

Further, such a double-peak warm interval[1] (*i.e.*, the 1920s and 1940s) also appears in the composite index from eight ice cores in West Antarctica (*i.e.*, measurements of water stable isotopes, either $\delta^{18}O$ or δD, as proxies of West Antarctic surface temperature) compiled by Schneider and Steig (2008, see their Figure 1a).

Significantly, Bronninmann (2009) called for a more thorough investigation of these early 20th century warming tendencies using regional temperatures because globally or hemispherically averaged data can hide physical insights. In heeding Bronninmann's (2009) call, this paper focuses on the 1920s and 1940s warming in the SAT record for the whole of China. Moreover, this warming is most likely naturally induced as Wood and Overland (2010) correctly remark that "greenhouse gas forcing is not now considered to have played a major role" for the observed warming in 1920s and 1940s in the Arctic and elsewhere. By contrast, the rapid warming of 0.5 °C/decade in the China-wide SAT data since the mid-1980s (Wang and Gong, 2000) has raised the possibility of early detection of the imprints of anthropogenic CO_2 global warming in the Chinese record over large geographical areas with middle to high elevations (>2000 m; namely the Qinghai–Tibetan [or Xi-Zang in Chinese] Plateau; see Wu et al. (2007) for a detailed physical discussion of the mechanical and thermal forcing by the Qinghai–Tibetan Plateau).

Regarding the potential warming from increasing atmospheric CO_2, several authors including Wang and Gong (2000) have noted that, the overall warming temperature history of China and the globe during the 20th century can be interpreted as a natural and persistent recovery from the Little Ice Age of AD 1300–1900 (*e.g.*, Zhu, 1973; Wang and Zhang, 2011; Hameed and Gong, 1994; Hsu, 1996; Wang et al., 2001; Yang et al., 2002; Soon et al., 2003; Wang et al., 2006; Akasofu, 2010; Ge et al., 2010; Lee and Zhang, 2010) for it is hardly conceivable for all the natural warming and cooling processes to cease suddenly in the late 20th century. Wang and Gong (2000) highlighted that "the warming time series in China indicates a sinusoidal variation over the past hundred years and is different than for global average."

Zhou and Yu's (2006) attempt to simulate the Chinese SAT using theoretical insight and climate modeling results have been met with both successes and failures. Figure 1 of Zhou and Yu (2006) shows the similarities and differences between the China-wide and Northern Hemisphere or globally averaged time series, including the very distinctive characteristic of the 1920s and 1940s warming in China. The key lesson of Zhou and Yu (2006) was the failure of any climate model, even by those forced with sea surface temperatures (SST), to capture the early warming of the 1920s as well as the insufficiency of atmospheric CO_2 forcing to explain the warming trend in the last half of the 20th century in China. Remarkably, Zhou and Yu (2006) encouraged international modeling groups to make model runs without forcing by well-mixed greenhouse gases, including anthropogenic CO_2 forcing.

This exemplifies critical insights that are required to understand all factors that affect climatic change. Such a call is scientifically significant in that it argues for the importance of understanding key natural processes that led to decadal and multidecadal variations found in the instrumental temperature records. In this paper, we use such an approach to investigate the role of the local and non-local forcing-feedback responses that are created by persistent variations in the incoming solar radiation at the top of the atmosphere and/or the modulated solar radiation reaching ground surface as represented specifically both by Total Solar Irradiance (TSI) and sunshine duration (SSD) indices, respectively (see more explanation of this in Section 2).

Recent progress reports from Chinese meteorologists and climatologists (*e.g.*, Zhao et al., 2005; Wang et al., 2006; Ding et al., 2007; Zhou et al., 2009a; Qian et al., 2010) placed similar emphasis on understanding natural factors of climate change as well as those resulting from anthropogenic forcing. In addition to anthropogenic emissions of gases and aerosols (Qian et al., 2007; Chung et al., 2010), it is clear that anthropogenic factors can result in local and regional climatic changes that were forced by significant land-use changes in China over the last 50 years. These effects include the damming of rivers, urbanization, irrigation, changing agricultural practices as well as the changing areas of forested and desert land surfaces (Zhou et al., 2004; Zhang et al., 2005; Ren et al., 2008; Yang et al., 2011). Although anthropogenic effects are not limited to just CO_2 emissions, it is expected that local and even regional temperature trends, such as the China-wide time series adopted in this study, will contain useful information for examining the physical processes involved. It is expected that several of the non-local and solar radiation-induced forcing-feedback mechanisms (for criticisms of studies of climate change that consider only a single causal factor, for example, the increase of atmospheric CO_2, see Soon, 2007; Pielke et al., 2009; Soon and Legates, 2010) will arise from these physical processes.

China is large geographically, has a long geological history, and exhibits strong seasonality in temperature variations such that processes that affect China must be critically examined. For example, the modeling study by Li et al. (2007) attributed the summer cooling trend over Eastern China since the 1950s to dynamical and thermal responses induced by regional anthropogenic sulfate aerosol forcing. But the quantitative effects of aerosol radiative forcing are highly uncertain in both sign and amplitude (Anderson et al., 2003; Kiehl, 2007; Knutti, 2008; Myhre, 2009, especially his Figure 1). Zhao et al. (2005) have

[1] Here we simply follow the double-warm-peak nomenclature described in Zhou and Yu (2006), but it is also plausible to view the 1920s through 1940s interval to be an overall warm interval, albeit with temporary cooler tendencies in between the 30-year-long time period.

outlined also the relevant meteorological and climatic processes that affect both the summer and winter monsoonal climate in China. These range from the El Niño/Southern Oscillation phenomenon (ENSO), snow cover and depth over the Tibetan Plateau, locations of the Siberian High, sea surface temperatures of the Indian Ocean, and the North Pacific Ocean, as well as atmospheric circulation indices such as the North Atlantic Oscillation, Arctic Oscillation, Western Pacific subtropical high, and even the Antarctic Oscillation (Zhao et al., 2005). Qian et al. (2010) raised an even more fundamental issue of the need for a proper reference frame, arguing for the use of a modulated annual cycle as opposed to the traditional anomaly of changes in the mean climatology over time. This provides for a more correct physics-based study of the multi-timescale variability of the surface air temperature variations in China. However, we concede at the outset that a full quantitative accounting of the SAT variations for all spatial domains and temporal scales in China is not yet possible.

We also refer to the cited references for discussions on interannual variations that are linked and correlated to the more dynamic, both local and non-local, indices and variables such as ENSO, winter and summer monsoonal circulation indices, Indian Ocean SST, and the western Pacific subtropical high. We await future studies using more sophisticated statistical analyses and tools (*e.g.*, Qian et al., 2010) to unravel the complex spatial–temporal patterns of the variability of the ten regional Chinese climate records that must necessarily involve the precipitation records (Wang et al., 2004) as well as various other natural and anthropogenic factors discussed above. An important discussion has been initiated by B. Wang et al. (2008) where the warming of the Tibetan Plateau over the past 50 years has been shown to enhance subtropical frontal summer rainfall in East Asia.

Finally, we wish to emphasize, as in Soon (2009; see clarification on pp. 148–149), that the focus here is on multidecadal variations/signals in the Chinese SAT records. We have largely avoided discussion on changes and variations on interannual and even decadal timescales that are required to account for variations in the solar UV radiation as well as the complex dynamic coupling involving the stratosphere and troposphere. To support our focus on multidecadal variations using only the instrumental thermometer records studied here, we supplement our discussion with available paleoclimatic evidence (Section 3 below). For the convenience of the reader, we list all acronyms in this paper in Appendix A.

2. Data and analyses

2.1. China-wide surface air temperatures

We adopt a primary surface air temperature record (SAT) for China (from 1880 to 2002) based upon the 10-region-averaged reconstruction by Wang and Gong (2000) and Wang et al. (2001, 2004). This homogenized SAT time series attempts to resolve issues associated with the urban heat island and other non-climatic discontinuities resulting from historical land use changes, though the impact of such issues still range between quantitatively significant (Portman, 1993; Zhou et al., 2004; Zhang et al., 2005; Ren et al., 2008) to relatively minor (Li et al., 2010).

Another source of SAT data for China is the construction by Lin et al. (1995) that provides time series data from 1873 to 1990. In addition to the annual-mean, this record also has monthly data from which seasonal averages can be computed. Seasonal details allow better analysis of the nature of variations in SAT, especially for a more detailed study of the 1920s and 1940s warming periods. The Lin et al. (1995) construction is also a 10-region-based SAT series but with a different station distribution and areal subdivision.

A third source of SAT data for China was obtained from the *Climate Data for Political Areas* project, based on the University of East Anglia Climatic Research Unit's (CRU) primary high spatial resolution ($0.5^\circ \times 0.5^\circ$) dataset (Mitchell et al., 2002). Overall, this dataset generally agrees well with the older analysis by Bradley et al. (1987). This is not surprising since both datasets likely utilized much of the same original data.

In considering the Wang et al. (2001, 2004), Lin et al. (1995), and Mitchell et al. (2002) datasets for China-wide SAT, it should be emphasized that the Mitchell et al. (2002) dataset is likely to be relatively independent from the other two. Zhao et al. (2005) has noted this and concluded that three out of four temperature time series of China they examined from the Mitchell et al. (2002) dataset were in relatively good agreement in terms of both interannual fluctuations and long-term variations. The latest comparison by Tang et al. (2009) yields a similar result. Some relevant differences are elaborated on and discussed in Section 3.

To provide a comparison with the instrumental temperature records, the SAT time series from 1871 to 2008 provided by the new 20th Century Reanalysis Project V2 (20CRv2) dataset (Compo et al., 2006, 2011) is also examined as a fourth data source. The 20CRv2 data has been obtained from the NOAA/OAR/ESRL PSD, Boulder, Colorado, USA, from their website at http://www.esrl.noaa.gov/psd. The strengths and weaknesses of this new 20CRv2 reanalysis dataset are discussed in Section 3 below.

Ma et al. (2008) recently evaluated the shorter SAT records from three other reanalysis products (ERA-40, NCEP-1, and NCEP-2 as defined by Ma et al. (2008); note that NCEP-1 represents NCEP/NCAR product from 1948 to the present, while NCEP-2 is a similar product covering only from 1979 to the present) with the homogenized observational data for China from 1958 to 2001 produced by the Climate Data Center of the National Meteorological Information Center of the Chinese Meteorological Agency. Ma et al. (2008) notes that the mean climatologies of all three reanalyses exhibit a cool bias in relation to the actual homogenized instrumental records (0.93 °C for ERA-40; 2.78 °C for NCEP-1; and 2.27 °C for NCEP-2). They found that this cool bias is related to an under-representation of the high elevation regions in western China. Similar concerns have also been raised by You et al. (2010). This result may not be entirely surprising, however, since Xia et al. (2006) has shown that surface solar radiation data from the NCEP/NCAR datasets exceeded direct surface observations by 55 W m^{-2} in northeast China, 80 W m^{-2} in southern China and by more than 100 Wm^{-2} in the middle reaches of Yangtze River (30°N, 107.5°E). The root mean square error (RMSE) varied from 61 to 89 W m^{-2} (note that a physical motivation and discussion of the surface solar radiation datasets are given in the next subsection). The key reason for such a large RMSE bias, according to Xia et al. (2006), is because the total cloud cover estimated by the NCEP/NCAR datasets was 10–20% less than satellite-retrieved coverage and because the NCEP/NCAR models did not include the effects of aerosols. We have no straightforward explanation on why the excess surface solar radiation in the NCEP/NCAR models leads to a cool, rather than a warm, bias in climatological temperature, as found in Ma et al. (2008), but the results perhaps suggest a certain degree of numerical tuning in the climate models.

To examine other teleconnection feedbacks on China-wide SATs, we also use the NCEP/NCAR reanalysis products, though only for the more recent time period (*i.e.*, 1979 to present) where satellite data are directly assimilated (*i.e.*, Kalnay et al., 1996; Powell and Xu, 2011; Powell and Xu, in press). Ma et al. (2008) discuss the NCEP/NCAR and European Centre for Medium-Range

Weather Forecast (ECMWF) datasets, and Powell and Xu (in press) note distinct differences in the stratospheric temperature response to solar forcing for pre-satellite and post-satellite data assimilation. Another physical linkage, noted by Sun et al. (2008), is a shift in linkages between the summer North Atlantic Oscillation[2] (NAO) and mid-eastern Asian SATs, with the summer NAO modes becoming located more eastward after 1979, coincident with the assimilation of satellite data.

Using the NCEP/NCAR datasets, Ma et al. (2008) confirmed a strong correlation between the mean annual China-wide SATs determined from the three reanalysis products from 1979 to 2001 (*i.e.*, $r=0.98$ for ERA-40, $r=0.94$ for NCEP-1, and $r=0.85$ for NCEP-2). As well, Xia et al. (2006) concluded that, despite the large biases in the mean climatology, solar radiation data from 1960 to 2000 in the NCEP/NCAR datasets exhibits increasing trends in northern, northeastern, and western China—consistent with decreases in cloud cover. Several other researchers have recommended that the ECMWF reanalysis dataset (ERA-40) is the best for China-based analyses (Frauenfeld et al., 2005; Ma et al., 2008; Zhao and Fu, 2009; You et al., 2010), mainly because ERA-40 assimilated surface observations when data were available while the NCEP reanalyses do not. However, the ERA-40 reanalysis produces erroneous temperature trends for the Arctic (Screen and Simmonds, 2011). As a result, all reanalysis datasets must be used with caution as all contain internal inconsistencies to some degree.

2.2. Solar radiation

The solar radiation proxies used here are based on the multi-proxy reconstruction of total solar irradiance (TSI) by Hoyt and Schatten (1993), as updated by Scafetta and Willson (2009).[3] Note that the absolute level of TSI since 1979 has been measured by satellite-based cavity radiometers to lie between 1360 and 1375 W m^{-2}. Resolving the uncertainty requires new measurements with more precise space-borne radiometers. Here, we have arbitrarily tuned the value of TSI so that the mean value from 1979 to 2008 is 1366.1 W m^{-2} (N. Scafetta 2009, private communication). Kopp and Lean (2011) suggest 1360.8 ± 0.5 W m^{-2} as the most accurate absolute value for TSI. The impact of this uncertainty in TSI on globally averaged or China-wide SATs is beyond the scope of this paper. It must be realized, however, that acknowledging the uncertainty in TSI is a prerequisite for the proper assessment of the dynamic evolution of the weather–climate system.

In light of several misunderstandings and inaccurate information concerning TSI (*cf.*, Kopp and Lean, 2011), further explanation is warranted. As no direct or continuous measurements of TSI exist prior to about 1979, the TSI before 1979 is reconstructed using information on proxies of solar magnetic activity and its variability, including empirical results from long-term monitoring of Sun-like stars (Baliunas et al., 1995).

Our reason for choosing the TSI reconstruction from Hoyt and Schatten (1993) is mainly because their work involves the most diverse types and ranges of proxy values for solar irradiance estimation. Hoyt and Schatten (1993) used five historical proxies: sunspot cycle amplitude, sunspot cycle length, solar equatorial rotation rate, fraction of penumbral spots, and the decay rate of the approximate 11-year sunspot cycle. Their assumption was that each of these slightly different proxies can most likely capture some part of the underlying factors responsible for modulating the solar magneto-convection-induced processes that affect TSI. Moreover, the TSI reconstruction of Hoyt and Schatten (1993) may facilitate a more self-consistent explanation of the China-wide SAT records because the solar equatorial rotation rate (see Figure 1 of Hoyt and Schatten, 1993) exhibits considerable variability in the early 20th century.

Another important issue concerning the TSI reconstruction is that the low-amplitude estimates favored by Lean et al. (2005), and indeed even by IPCC AR4 (2007), were based on computer modeling by Wang et al. (2005). We note that the magnetic flux transport model that was used was not designed to model irradiance changes or to assess the solar energy budget. Furthermore, this model does not even contain a radiative transfer routine, which is essential to a proper description of solar physics. Thus, the Lean et al. (2005) reconstruction is limited in its ability to describe variations in TSI. Furthermore, direct empirical evidence from the studies of Sun-like stars (see Zhang et al., 1994) supports the use of the Hoyt and Schatten (1993) reconstruction. Interested readers are referred to end note #4 of Soon (2009) for a more detailed explanation of why the discussion of TSI variability in Section 2.7 of the AR4 Working Group I report of IPCC (2007) seems neither objective nor inclusive. It also is relevant to note that in Shapiro et al. (2011), the amplitude of total solar irradiance change between present and the Maunder Minimum interval was determined to be 6 ± 3 W/m^2; a value significantly larger than estimates by several authors but in good agreement with the estimate by Zhang et al. (1994). This latest result supports the amplitude of total solar irradiance series shown in the present study.

Another unique proxy for solar radiation is the Japanese sunshine duration (SSD) data recently deduced from the Jordan and Edo sunshine recorders, and calibrated with "global" radiation estimates using surface thermopile pyranometers (Stanhill and Cohen, 2008). By definition, surface sunshine measurements represent conditions when direct solar beam irradiance exceeds 120 W m^{-2} and when the solar disk is more than 5° above the horizon unobstructed by clouds, mist, fog or haze. Such direct measurements are widely available for many locations but it is rare for a regional record (aggregated from 65 stations/locations across Japan) to represent continuously the full time period from 1890 to 2002 as this SSD dataset does. Although Stanhill and Cohen (2008) also provided calibrated annual-mean values of "global" radiation that vary from about 140 to 160 W m^{-2} over the full 113 years of the record, we only use here the original ground solar radiation data, measured in units of sunshine duration as the total number of hours in a year. A further caution is that the Japanese SSD parameter should not be viewed as climate "forcing" variable *per se* bur rather it is mostly probably a complex expression of multi-factorial forcing-feedback parameter which is yet to be fully resolved.

In addition, two other reasons exist for including this Japanese SSD record. Many studies (Stanhill and Cohen, 2001; Liu et al., 2002; Qian et al., 2007; Wang et al., 2007; Hinkelman et al., 2009; Norris and Wild, 2009; Ohvril et al., 2009; Ruckstuhl and Norris, 2009; Wild et al., 2009) have examined plausible causal factors for changes in atmospheric transmissivity and these arguments will not be discussed here. Nevertheless, it is important to avoid speculation on various short-term trends and tendencies in the sunshine duration datasets for China. Figure 5 of Li et al. (2005), for example, shows an interesting inverse correlation ($r=-0.68$) between March SAT and total cloud amount over the Sichuan basin (27°N–32°N, 103°E–108°E).

Other solar radiation datasets are available for China (*e.g.*, Li et al., 1998; Kaiser and Qian, 2002; Che et al., 2005; Xia et al., 2006; Shi et al., 2008; Norris and Wild, 2009) but none of these

[2] Although not a focus in this paper, we note that there is a hint of multidecadal modulation in the summer NAO index; a rough correlation exists between the total solar irradiance index adopted here and this North Atlantic atmospheric circulation index.

[3] There are unresolved issues regarding which TSI datasets to adopt for the 1979-present interval (see, for example, Domingo et al., 2009; Frohlich, 2009; Krivova et al., 2009; Wenzler et al., 2009; see also Kopp and Lean, 2011), but we emphasize the focus on multidecadal variations in this study.

cover the entire 20th century except for Taiwan (Liu et al., 2002). However, the relatively good quality-controlled SSD Japanese dataset may be useful to estimate the role of the near-surface energy budget in modulating the large-scale land–sea diabatic heating that affects the larger region of China, East Asia, and Western and Central North Pacific. For example Lindzen and Choi (2011) have shown that the role of clouds as both forcing and feedback parameters on most climatic timescales remain largely difficult to quantify.

2.3. Correlations of Japanese SSD with other spatial domains

Stanhill and Cohen (2008) have found a high correlation between the Japanese SSD dataset and Northern Hemisphere averaged SAT (monthly correlations between 0.62 and 0.69). In general, our research confirms such statistical correlations ($r=0.62$) with the annual series, and improving substantially ($r=0.85$) after application of an 11-year rectangular filter.[4] Physical insights on these correlations are examined in Section 3 in the context of China-wide SATs. Figure 1 of Ohmura (2006) shows, however, that the longer surface global radiation records at Stockholm and Wageningen display an "increasing trend [in surface solar radiation] was already set in the 1920s." Ohmura (2006) further quantified the increase of the global radiation at the two sites between 1922 and 1952 to be about 20 W m^{-2}. The atmospheric column transparency coefficient deduced by Ohvril et al. (2009) over the Estonia–western Russia region, especially those at Pavlovsk and Tartu-Toravere, also suggested greater transmission of direct solar beam irradiance during the 1920s–1940s relative to the 1980s. Stanhill and Cohen (2005) offered evidence for a relatively lengthening of the sunshine duration for data averaged over 106 sites in the United States, which peaked in the late 1920s–early 1930s, thereby adding credence to the task of providing realistic constraints on the warm periods in China during the 1920s–1940s. Although the focus here is on the 1920s through 1940s interval, disagreements between peaks and variations of SSD for various locations and regions at other time intervals should be acknowledged and carefully studied as well.

Consequently, the Japanese SSD dataset may be considered as a valid proxy for surface radiation and provides constraints on teleconnections with China via the marine near-surface energy budget for offshore Japanese waters and the adjacent central North Pacific Ocean, and perhaps even for the tropical and subtropical western Pacific. Pavlakis et al. (2008), for example, emphasized that surface shortwave radiation for the off-equatorial western Pacific region (7°N–15°N, 150°E–170°E) was a leading variable of the Niño 3.4 SST index by about seven months, with the potential for ENSO forecasts.

2.4. Summary

In our analysis of variations and factors that drive China-wide SAT, we adopt a simple direct correlation analysis of solar and climatic variables, with an emphasis on the persistent multidecadal co-variation of solar-terrestrial relationships. Existing papers have revealed multidecadal oscillations in China-wide precipitation data (Wang et al., 2004; Ding et al., 2007), summer rainfall (Zhu and Wang, 2002; Ding et al., 2007) and the East Asian summer monsoon (Guo et al., 2004) that can be linked to variations in solar activity (see also Wang and Zhang, 2011; Hameed and Gong, 1994; Liu et al., 2009; which includes a discussion on the evidence for solar-related climatic influences on the bicentennial timescale). Here, focus is on the multidecadal variations in SAT and plausible direct evidence for the connection to solar activity using TSI and SSD indices is sought. Wavelet transforms are used to discern the time–frequency patterns (see Appendix B for the description of these methods) of Chinese SATs and the solar radiation indices.

3. Results and discussion

Annual-mean SAT time-series for China are presented from 1870 to 2008 by (1) Peking University (Wang et al., 2001, 2004), (2) Chinese Academy of Meteorological Science (Lin et al., 1995), (3) CRU (Mitchell et al., 2002), and (4) for 1871–2008 from 20CRv2 dataset (Compo et al., 2011). Although good agreement exists among these four sources, especially post-1979, large qualitative and quantitative differences exist prior to 1979 (Fig. 1b).

The 20CRv2 reanalysis product is based upon an assimilation of surface pressure data, with given monthly sea surface temperature (SST) and sea ice distributions, as boundary conditions (Compo et al., 2006, 2011). However, numerical experiments by Zhou and Yu (2006) were unable reproduce the observed double-peak in SATs in the 1920s and the 1940s (see Fig. 1a) when driving an atmospheric climate model with the same SST and sea ice boundary conditions from 1870 to 2003 as in 20CRv2. This suggests that the coupled ocean–atmosphere system—its processes and dynamics—are more complex than the model represents. In particular, Lu et al. (2006) demonstrated the importance of coupled atmosphere–ocean feedbacks in the western Pacific and Indian Oceans and showed that the tropospheric temperature changes in Eurasia (see below for the detailed discussion of this variable) can explain how the Atlantic Multidecadal Oscillation (AMO) modulates the Asian summer monsoon.

Although they are not entirely independent, a rough qualitative agreement exists between the existence of the warming in the 1920s and 1940s in both the CRU datasets (Mitchell et al., 2002; Bradley et al., 1987; see especially their Figure 7). Moreover, Bradley et al. (1987) demonstrated that the 1920s warming was largely a result of a dramatic increase in spring and summer temperatures (see their Figure 9). This is independently confirmed by the seasonal SATs of Lin et al. (1995) where the 1920s exhibit a more persistent warming during the summer relative to the winter and where the signal is less coherent (their Figure 4). This characteristic is confirmed also by the monthly data provided by Mitchell et al. (2002). Similarly, the spring and summer warming of the 1920s (and to a much lesser extent during autumn) is also shown by Jones et al. (2008; their Figure 8). This spring–summer warming of the 1920s has particular relevance to our discussion of plausible physical explanations of the interconnections between solar radiation and China-wide SATs as well as teleconnections elsewhere, as explained below.

A note of caution is required regarding the use of China-wide SATs for the entire 20th century from the reanalysis data. Previous papers (*e.g.*, Ma et al., 2008; Zhao and Fu, 2009) have raised concerns about data accuracy even over the latter portion of the 20th century (*i.e.*, post-1979) because of issues related to spatial coverage of the data records. Tang et al. (2009) compared five different time series from 1873 to 2007 of China-wide SATs and caution that some of these datasets have incomplete spatial coverage which limits the data to just eastern China before 1920. We agree with these assessments.

In addition, our intercomparison (Fig. 1b) agrees well with the independent findings of Wen et al. (2006) who report that the CRU dataset for China (a slightly different version than that used here) is highly correlated with the SAT of Wang et al. (2001, 2004).

[4] We are however unsure on how to interpret the correlation of a local and regional variable like the Japanese SSD with a hemispheric-scale parameter like Northern Hemisphere SAT.

Wen et al. (2006) further commented that the differences were greatest in the 1920s, when the CRU data underestimate the warming in China and thus overestimate the overall 20th century warming trend.

Agreement among the three China-wide temperature series (Fig. 1b) from Wang et al. (2001, 2004), Lin et al. (1995), and Mitchell et al. (2002) during the 20th century is within acceptable limits—R^2 ranges from 0.55 to 0.75 for the yearly data and as high as 0.94 between the Wang et al. (2001, 2004) and Lin et al. (1995) records when smoothed with an 11-year rectangular filter to highlight multidecadal-scale variations. This suggests that the warmth of the 1920s and 1940s in China was real and not a result of data reconstruction biases and errors. A physical explanation for this warmth may be the large change in the East Asian Monsoon Index (Figure 3.35 of the Working Group I report of the IPCC (2007)) from a low between 1907 and 1910 to a high in the 1920s. The East Asian Monsoon Index measures the zonal land–sea thermal contrast (Guo et al., 2004; Zhou and Zou, 2010) but the meridional gradient should also be considered (as discussed in Zhou and Zou, 2010; see further discussion below). It is also relevant to note that in the reconstruction of seasonal temperatures over north China using historical records of snow, frost, sea ice, and excessive rainfall since AD 1380, Wang (1990) demonstrated the prominence of the 1920s and 1940s warm periods for spring, summer, and autumn (see Figures 2 and 3 of Wang 1990).

Based on this extensive evidence—ranging from the Arctic to the Antarctic—the relative warm decades of the 1920s and 1940s were associated with large and significant natural shifts and episodic variations as part of multidecadal-scale oscillations. But much more research remains to unlock the full interconnection and phasing of these influences across all major climatic regions around the globe. Consequently, the substantial warming of the 1920s and 1940s in China still needs to be properly placed in a global context.

The time–frequency wavelet spectra and other amplitude–frequency-phase information on the annual-mean Chinese SAT from 1880 to 2002 are shown in Fig. 2. Here, the focus is on SAT variability at multidecadal timescale. The wavelet transform has been used to study Sun–climate relations for both the study of changes in dominant periodicities and the possible separation of different dominant timescales (*i.e.*, Soon, 2005; Weng, 2005). Appendix B provides a detailed presentation of the wavelet transform calculations.

The results of Fig. 2 suggest a dominant and persistent oscillation of about 40–80 years is present across the whole time-series. Despite the shortness of the Wang et al. (2001, 2004) SAT record, the dominance of SAT variability at a 60- to 65-year timescale does not appear to be unique to China. In fact, such a dominant timescale of climatic variability has been discussed for the North Atlantic and Eurasia (Schlesinger and Ramankutty, 1994), the North Pacific and North America (Minobe, 1997), and even the Indian Summer Monsoon rainfall record (Agnihotri and Dutta, 2003). Wang and Zhang (2011) reported similar multidecadal variation signals (*i.e.*, around 73 and 60 years) in their new tree-ring width record from the transitional zone between semi-humid and humid climatic region of the Sygera Mountain at southeast Tibet. By way of explanation, Kirby et al. (2002) described how the contraction and expansion of the winter circumpolar vortex may modulate multidecadal (*i.e.*, our 60- to 65-year scale) and longer timescale signals as revealed in their stable oxygen and carbon isotope records. Weng (2005) also analyzed sea surface temperature variations from 1870 to 2004 over the North Pacific Ocean (40°N–60°N; 140°E–120°W) and noted the appearance of a 60-year periodicity after about 1940. Finally, although we do not agree with the conclusion of Knudsen et al. (2010), those authors show evidence for notable 60-year scale oscillations in the $\delta^{18}O$ record from Lake Chichancanab of Yucatan Peninsula, the Ti record from Cariaco Basin as well as the coral $\delta^{18}O$ record from southwestern Puerto Rico through the last 8000 years.

Soon (2009) summarized the evidence from paleo-SAT and precipitation proxies for multidecadal climatic oscillations over periods ranging from the last millennium to the entire Holocene in his Table A1. We discuss here further the physical mechanisms and processes that control the initiation, timing, speed, and longevity of these multidecadal climate variations. We note too that separation of some multidecadal-scale patterns from longer centennial- and bicentennial-scale solar variability is difficult to achieve because of potential sampling and aliasing problems. Nevertheless, evidence exists on multidecadal and multicentennial timescales for variations in the intrinsic properties of the Sun and its magnetism which, in turn, are variable and ever-changing (*e.g.*, Yoshimura, 1979; Ikhsanov and Vitinskii, 1980; Ding et al., 1983; Xu, 1990; Du, 2006; Kane, 2008; Miyahara et al., 2008; Heristchi and Mouradian, 2009; Kollath and Olah, 2009; de Jager et al., 2010; Usoskin et al., 2010). Kollath and Olah (2009), for example, specifically noted the quasi-continuous lengthening in

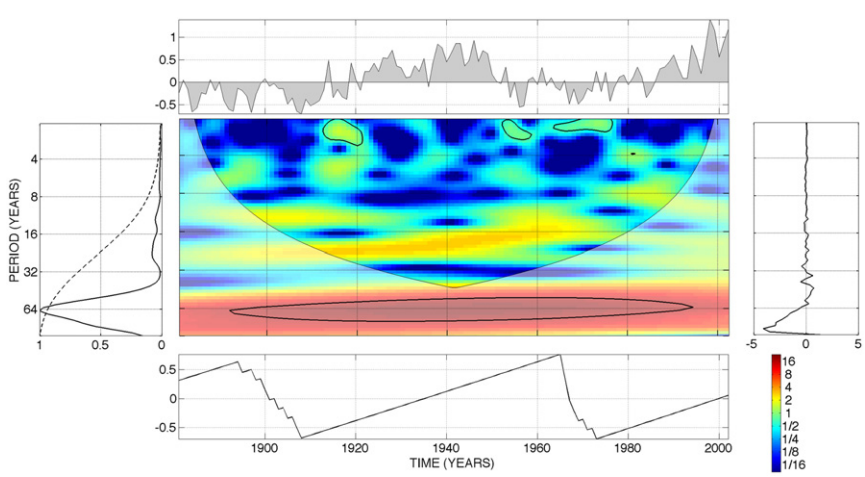

Fig. 2. Wavelet transform analysis of the China-wide surface air temperature series (shaded area in top panel) from 1880 to 2002 by Wang et al. (2001, 2004). The center panel gives the time–frequency values of the wavelet power. The left panel shows the global spectrum of the wavelet power averaged over time. Dashed lines represent the significance level of the global spectrum and are referenced to the power of red noise level at the 95% confidence interval. The right panel shows the global phase information while the bottom panel gives the instantaneous phase for the selected multidecadal oscillatory scale of about 60-years.

the multidecadal-centennial oscillatory scale from a periodicity of about 50 years in 1750 to about 130 years by 1950.

Comparison between the China-wide SAT of Wang et al. (2001, 2004), the TSI series (Fig. 3), and the Japanese SSD series (Fig. 4) shows that high correlations exist with explained variances (*i.e.*, R^2) of 71% and 53%, respectively, for the 11-year smoothed time series. Observed (unsmoothed) annual-mean data exhibits more variability with explained variances dropping to 42% and 36%. Moreover, the warming in China during the 1920s and 1940s are not dissimilar with parallel changes in TSI and SSD so that changing solar irradiance and the solar radiation reaching the surface cannot be excluded as important factors that may have partly driven/forced these two warming episodes. Note again that the science on atmospheric transparency and changes in cloudiness has not yet developed to a level that direct connections between TSI and SSD can be explained (see *e.g.*, Lindzen and Choi, 2011), and nor are we sure as to how representative the Japanese SSD are of the larger East Asia region (but see Fig. 5).

It is unreasonable to dismiss these correlations as a statistical coincidence without a physical cause. Rather, this research, which is based on empirical results (Figs. 3 and 4), demonstrates that a direct Sun–climate connection exists, manifest by its impact on SATs. The Japanese SSD data (Fig. 4) circumvent the complicating issues related to variations in cloud and atmospheric transmissivity, on any timescale. These empirical relationships enhance our physical understanding of climate variability on multidecadal time scales over China. However, as noted above, the Japanese SSD data should not be interpreted as a climatic "forcing" *per se* since this observed quantity is most likely a complex manifestation of various forcing and feedback interactions inherent in the weather–climate system.

Next, we propose two broad scenarios to cover the physical mechanisms that may best describe air–sea processes in the East Asian region. First, we suggest that the observed multidecadal modulation of air temperature by solar irradiance, both at the top of the atmosphere (TSI) and that reaching the ground (Japanese SSD), causes large-scale land–sea thermal contrasts and affects atmospheric circulation. Variations in both TSI and SSD may modulate the land–sea thermal contrast between the continental landmasses and the key centers of action in the tropical and subtropical Pacific Ocean (van Loon et al., 2004; Zhou et al., 2009a,b; Zhou and Zou, 2010). This effect arises from the differential heat capacity and thermal inertia of the land, air, and ocean. Zhou et al. (2009b) showed that changes in the position and location of the western Pacific subtropical high strongly affected the East Asian Summer Monsoon (see also Gong and Ho, 2002). They pointed out that changes in the position of the high are, in turn, controlled by convection and precipitation in the Indian Ocean and western Pacific warm pools and the concomitant diabatic heating variability. Zhou and Zou (2010) further studied the large-scale land–sea thermal contrasts using indices that account for both the zonal and meridional gradients of thermal and mechanical forcings and showed that meridional thermal contrast is better simulated by fixed SST models than are zonal

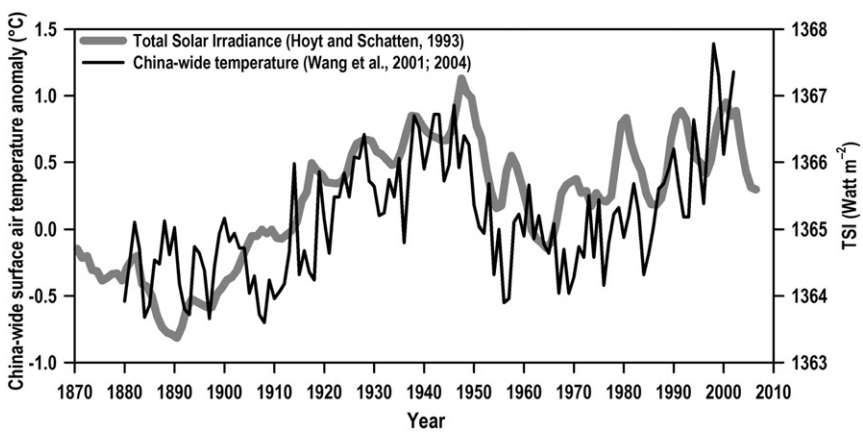

Fig. 3. Annual-mean China-wide surface air temperature time series by Wang et al. (2001, 2004) correlated with the estimated total solar irradiance TSI of Hoyt and Schatten (1993; with updates) from 1880 to 2002.

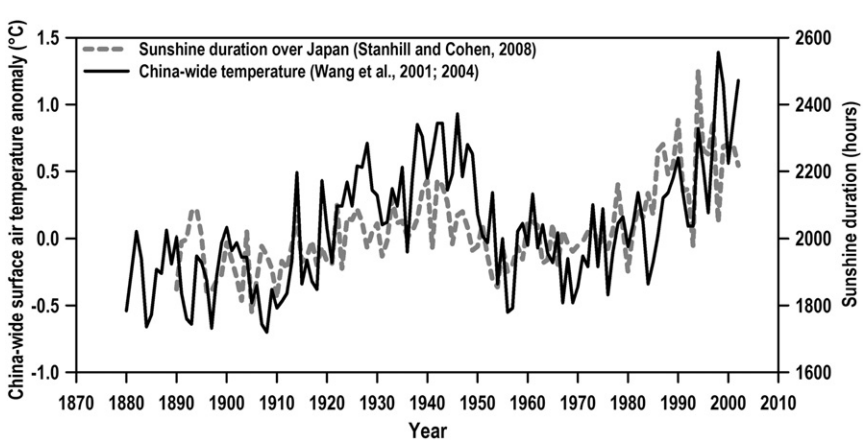

Fig. 4. Annual-mean China-wide surface air temperature time series by Wang et al. (2001, 2004) from 1880 to 2002 correlated with the Japanese sunshine duration of Stanhill and Cohen (2008) from 1890 to 2002.

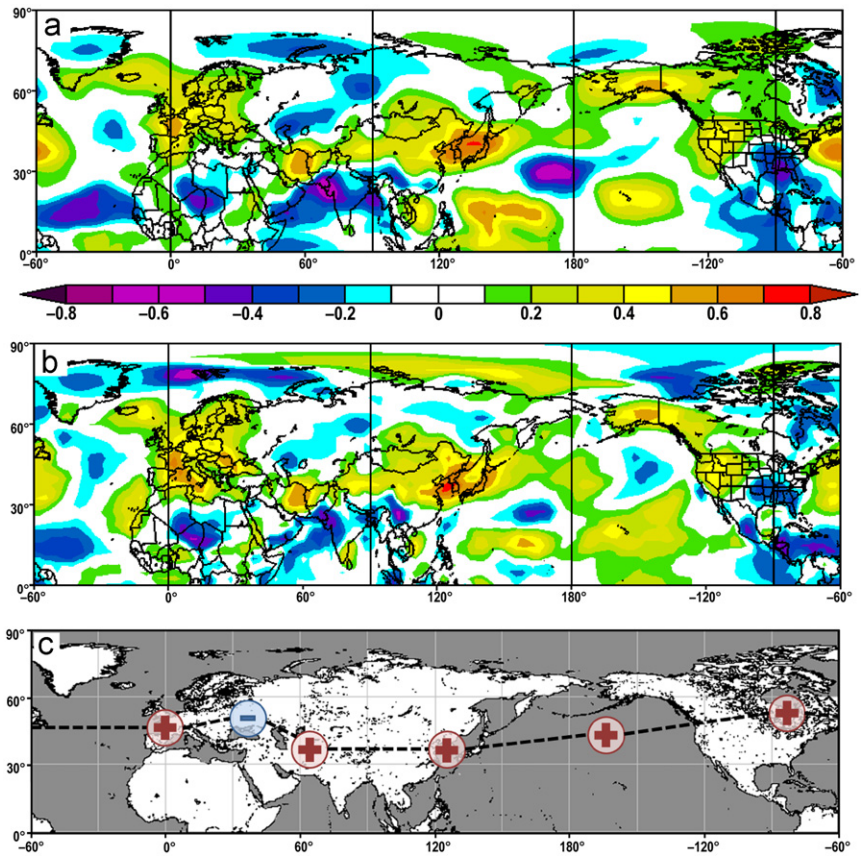

Fig. 5. Correlation between Japanese sunshine duration time series and the NCEP/NCAR reanalysis (a) (near-surface) air temperature at 850 hPa level and (b) surface air temperature over the 1979–2002 interval. (c) The recurrent Circum-global Teleconnection (CGT) pattern of the summertime mid-latitude circulation identified by Ding and Wang (2005) (adapted from their Fig. 1c).

contrasts. Zhou and Zou (2010) also found difficulty in modeling changes in continental sea level pressures which adversely affects the ability to simulate the land–sea thermal contrast that is required to account for the variability in the East Asian summer monsoon. Consequently, changing solar radiation on multidecadal timescales must impact China-wide SATs which cause the modulation of thermal and other properties at both local and regional scale (as suggested by Figs. 3 and 4).

These solar-radiation-induced changes may either reinforce or negate teleconnections between the Arctic–North Atlantic and the East Asian and Indian Monsoonal regions. Soon (2009), who focused on the Arctic and North Atlantic regions, has demonstrated that variations in TSI at multidecadal to multicentennial timescales cause differential interactions between the tropical and extra-tropical regions that modulate the equator-to-Arctic transport of heat and moisture, thus markedly affecting the climate and hydrology of the Arctic. The evidence for climate modulation by changes in TSI for the North Atlantic and North Pacific Oceans includes (1) the equator-to-pole temperature gradients, (2) the variable strength of the Atlantic meridional overturning circulation (MOC) or the thermohaline circulation (THC), (3) the shift and modulation of the Inter-Tropical Convergence Zone (ITCZ) and the tropical Atlantic Ocean, and (4) the intensity of the wind-driven subtropical and subpolar gyre circulation.

Multidecadal to centennial modulation of freshwater budgets and the Atlantic thermohaline circulation by TSI ultimately affects tropical and extra-tropical climate processes, including ENSO (Dong et al., 2006; Timmermann et al., 2007), the Indian summer monsoon (Goswami et al., 2006; Feng and Hu, 2008; Li et al., 2008; Rajeevan and Sridhar, 2008; Yadav, 2009), and the East Asian summer and winter monsoons (Lu et al., 2006; Li and Bates, 2007; Wang et al., 2009).

For example, Wang et al. (2009) have shown that atmospheric impulses originating in the North Atlantic propagate eastward via a Circum-global Teleconnection (CGT) transmitted by the North African–Asian Jet. The resultant complex geographical and seasonal patterns (Branstator, 2002; Enomoto et al., 2003; Selten et al., 2004; Wakabayashi and Kawamura, 2004; Watanabe, 2004; Ding and Wang, 2005; Sato and Takahashi, 2006; Sun et al., 2008; Kosaka et al., 2009; Lin, 2009; Yang et al., 2009; Ding et al., 2011) affect the tropospheric thermal balance above the Eurasian continent and Tibetan Plateau (see Figure 1 of Wang et al., 2009). Such thermal modulation of the atmosphere above the Eurasian continent during the warm phase in the Arctic–North Atlantic region will strengthen the Asian summer monsoon but weaken the winter monsoon. Another key branch of the summer circulation teleconnective pathway, popularly labeled the Tokyo–Chicago Express, connects the East Asian Monsoon region to North America (Nitta, 1987; Chen, 2002; Lau and Weng, 2002; Lau et al., 2004). Similarly, other recurrent Circum-global Teleconnection pathways associated with the South Asian Jet operate during boreal winters, for example, connecting the source region in South Asia with the central North Pacific and as far as the East Coast of the United States and the Gulf of Mexico (Branstator, 2002; see also Honda et al., 2005). Though such issues are beyond the direct scope of this present research, the related CGT relations and impacts for the Indian Summer Monsoon have been discussed in detail by Ding and Wang (2005), Rajeevan and Sridhar (2008), Li et al. (2008), Yang et al. (2009), and Ding et al. (2011).

Another plausible physical pathway for transmitting multidecadal signatures in the North Atlantic to the Central North Pacific has been presented by Zhang and Delworth (2007) and Wu et al. (2011). Their plausible scenario relies upon the modulation of atmospheric eddy heat transport and upper level eddy vorticity flux by the AMO, followed by atmospheric teleconnection and internal adjustment of the coupled ocean–atmosphere processes in the Central North Pacific and Kuroshio Current region, with changes in AMO leading those in the PDO by eleven to thirteen years. On the other hand, Wu et al. (2011) showed the alternate possibility that the PDO leads the AMO by one year. It is important to note the additional complexity that data lags and leads can cause for any interpretive studies when they are associated with multidecadal and centennial scales climate variations.

We now consider what changes in summer mid-latitude circulation patterns might be responsible for the increased Chinese SATs during the 1920s, given the persistence of coupled ocean–atmosphere interactions over the North Pacific summer (rather than winter) that have been recorded by Zhang et al. (1998) and Norris et al. (1998). Ding and Wang (2005, p. 3495) place an emphasis on the modulation of SAT by solar radiation through a recurrent summer CGT circulation pattern and note "because of the existence of the pressure anomaly with a barotropic structure, the shortwave radiation fluctuation that is associated with increased or decreased rainfall or cloud coverage may play a central role in general surface temperature change."

We illustrate here (Fig. 5) the spatial patterns of correlation between the NCEP/NCAR's air temperatures at the 850 hPa level, SAT and the Japanese SSD for the satellite assimilation period (1979–2002). The near-surface coupled air–sea processes that control these correlations are apparent also in Meehl et al. (2008, Figure 4), who show (i) that a globally averaged solar forcing at the top of the atmosphere of 0.2 W m^{-2} is too small to affect the climate system locally, but that nonetheless (ii) the net solar flux at the surface can often vary by at least a factor of five to ten times larger than at the top of the atmosphere. This result occurs because of the presence of cloud-free regions in the subtropical Pacific, combined with coupled air–sea mechanisms that ultimately create even larger cloud-free regions.

Understanding the role of SSD on various air–sea interactive processes and dynamics reinforces the results of Ding and Wang (2005) in their study of summer CGT patterns and surface SATs. The interactions between the NCEP/NCAR 850 hPa air temperatures (Fig. 5a) and SATs (Fig. 5b) with the Japanese SSD are located at one of the six main action centers (see Lin, 2009 for the possibility of CGT patterns with zonal wavenumber 6) of the CGT. Indeed, one can identify five of these six centers in the correlations between the 850 hPa temperatures/SATs and SSD. A slight difference in the location of the COA in the central North Pacific and the apparent absence of the one over North America (Ding and Wang, 2005) warrant further investigation. But given the persistent signal present which extends from the upper troposphere (around 200 hPa level) to the surface, the results in both Fig. 5a and b are physically interesting.

Two of the positive correlation centers in Fig. 5a and b differ slightly from the COAs of CGT in Ding and Wang (2005): one lies in the Gulf of Alaska region and the other in the Northwest Atlantic Ocean (which shows up more clearly in the 850 hPa level temperature; Fig. 5a). We note that the Atlantic center is roughly co-located with the Northwest Atlantic SST center over at 30°N–40°N and 40°W–65°W which Rajeevan and Sridhar (2008) found to be dynamically relevant for Indian summer monsoon rainfall. Fig. 5a also suggests the presence of strong negative correlation centers in the western central Pacific and in northwestern India within the 20–30°N zonal band (these are distinct from the main summer CGT Jet band, which lies slightly further north; see for example Figure 2a of Ding et al. (2011)). These various features all require further study.

An additional positive correlation center at about 10°N–20°N and 130°E–170°E is apparent between the NCEP/NCAR 850 hPa temperatures and the Japanese SSD data (this center is more prominent at the 850 hPa level than at surface; Fig. 5a) and also between the NCEP/NCAR SAT and SSD data (Fig. 5b). The correlation in Fig. 5b, perhaps coincidentally lies near the center of dynamic action for the East Asian summer monsoon in the western Pacific subtropical high region (*e.g.*, Nitta, 1987; Zhou et al., 2009b). In turn, this positive SAT–SSD core region in the subtropical western Pacific overlaps with the key region of ENSO 'predictability' around 7°N–15°N and 150°E–170°E, as discussed by Pavlakis et al. (2008).

The significance of Fig. 5 is that it demonstrates that during summer, the upper tropospheric CGT circulation pattern (at 200 hPa) interconnects with the variability of the SATs across the entire Northern Hemisphere mid-latitudes. The existence of a connection between summer CGT and SATs leads to a physical meaning based on the empirical correlations of Figs. 3 and 4 at multidecadal to centennial timescales. If independent corroboration can be secured, Fig. 5 is strong evidence of the direct impact of ground solar radiation on the SAT variations in the East Asian monsoon region, although further evidence is required to confirm the relationships for TSI.

Cross wavelet transform analyses between Chinese SATs and both TSI (Fig. 6) and Japanese SSD (Fig. 7) identify strong multidecadal- and centennial-scale covariability. The global spectrum of the cross wavelet power between Chinese SAT and TSI (Fig. 6) shows that the most prominent periodicity, with a confidence level above 95%, is around 60–65 years. This periodicity covers the full time interval (1880–2002) as shown by cross wavelet power in the central panel. The arrows at 0° (horizontal right) indicate that both phenomena are in phase, and imply also a linear relationship between the two time series. System response time is represented by the instantaneous relative-phase in the 60-years oscillatory scale (calculated in the bottom panel, Fig. 6). The delay time (system response) has a maximum of about a month, which implies the presence of a TSI-induced co-variation of Chinese SAT on the 60-year timescale, although such lead times are within the margins of error for both data series. Fig. 6 also suggests synchronization in frequency, amplitude and phase for the 60-year oscillatory scale. Overall, Fig. 6 implies the presence of strong coupling between Chinese SAT and TSI series.

Another cross wavelet transform result (Fig. 7) reveals similar coupling between Chinese SATs (shaded area in the center-top panel) and the Japanese SSD (solid line) from 1890 to 2002. The global spectrum of the cross wavelet power (left panel) again identifies that the most prominent periodicity is about 60 years. This periodicity is present over the entire time period (1890–2002), as shown in the central panel of cross-wavelet power. Again, the arrows at 0° (horizontal right) indicate that both phenomena are in phase and imply a linear relation between Chinese SAT and Japanese SSD. The global phase information in the right panel shows little variability in the periodicity of 60 years, which indicates synchronization and strong coupling. The time of system response indicated by the instantaneous relative-phase information within the 60-year timescale (bottom panel) and the delay time (system response) exhibits a maximum delay of about one and a half months. This result suggests that variations in SSD around Japan result in variability in Chinese SATs on the same 60-year timescale as described above.

Thus, the existence of synchronization in frequency, amplitude and phase between Japanese SSD and Chinese SAT on a 60-year periodicity implies a strong coupling between these two measures at the climatically important multidecadal timescale.

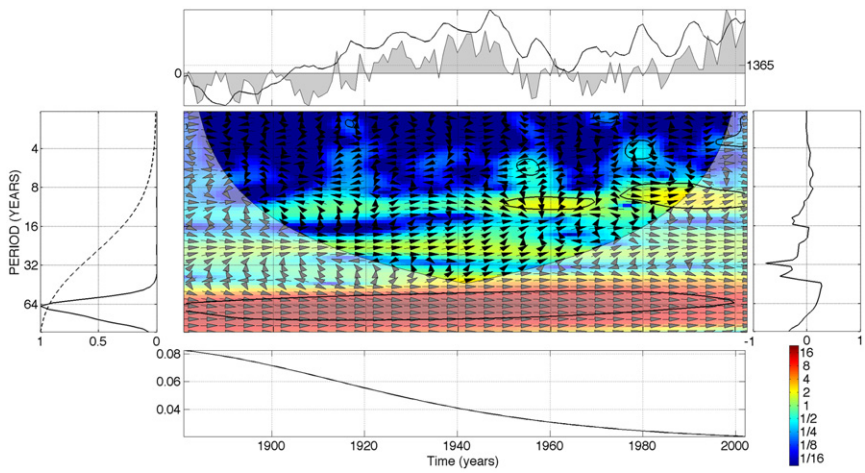

Fig. 6. Results of the cross wavelet analysis for the co-variations of China-wide surface air temperature (shaded area in the top panel) and total solar irradiance (solid line in the top panel) time series from 1880 to 2002. The left panel shows the global spectrum of the cross wavelet power. The dashed line represents the significance level of the global spectrum and refers to the power of red noise level at the 95% confidence interval. The right panel shows the global relative-phase relationship between the two time series. The center panel shows the cross wavelet power and the bottom panel gives the time delay between the two time series for the 60-year-scale oscillation. Descriptions of our calculations are given in Appendix B.

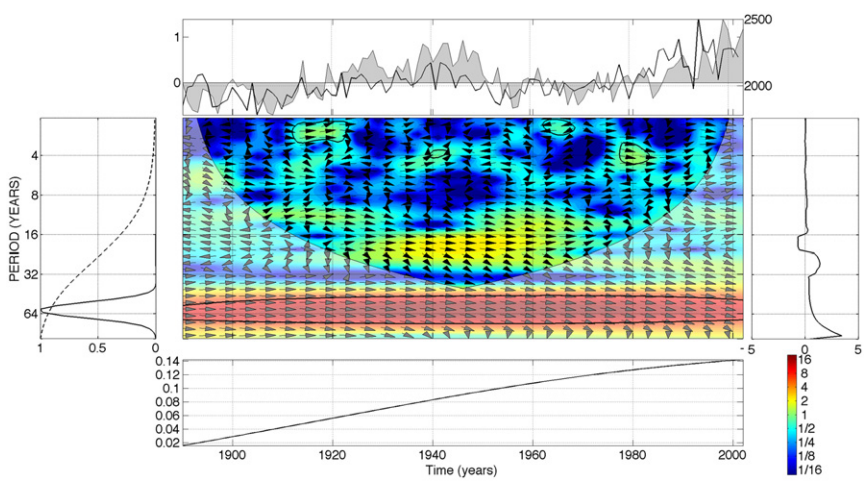

Fig. 7. Results of the cross wavelet analysis for the co-variations of China-wide temperature (shaded area in the top panel) and Japanese sunshine duration (solid line in the top panel) time series from 1890 to 2002. The quantities shown in the other four panels are as described in Fig. 6.

4. Conclusion

We have presented evidence that China's surface air temperatures during the 20th century were influenced by variations in both the incoming solar irradiance and ground surface solar radiation. This argues for a significant role for Sun–Earth relationships as a natural cause for observed multidecadal climate oscillations. Such an argument is distinct from, and also an alternative to, the allocation of a dominant anthropogenic cause for the variation in Chinese SATs since 1980. Both empirical evidence and statistical correlations demonstrate a role for natural climate fluctuations caused by variable solar forcing as an explanation for observed Chinese SATs. Pursuing a better understanding of the relevant physical processes and linkages, and especially clarifying their nature on multidecadal to centennial timescales (*cf.*, Fig. 5), should prove to be fruitful avenues for future research.

We therefore agree with Zhao et al. (2005) that natural causes cannot be excluded as a cause for changes in China's SAT, despite several published studies that favor anthropogenic causes. Our research goes beyond these studies in that we have shown that solar influence on Chinese SATs at multidecadal and longer timescales cannot be discounted, as also suggested by Weng (2005). Any comprehensive assessment of climate forcing *must necessarily* include natural variability, including solar variability, in addition to anthropogenic causes. Especially important is to elucidate the role played by anthropogenic aerosols in the modulation of near-surface shortwave and longwave radiation.

Acknowledgments

We thank Dr. TianJun Zhou for sharing with us the 10-region averaged Chinese temperature record of Professor Shao Wu Wang of Peking University and Drs. Gerald Stanhill and Shabtai Cohen for sharing their compilation of the Japanese sunshine duration data. We also thank Drs. Gene Avrett, Bob Carter, and two anonymous referees for a careful reading of the manuscript and suggesting important improvements.

Appendix A. Acronyms

20CRv2	20th Century Reanalysis Project V2
AMO	Atlantic Multidecadal Oscillation

AR4	UN's IPCC Fourth Assessment Reports (2007)
CGT	Circum-global Teleconnection
COAs	centers of (climatic) action
COI	cone of influence
CRU	Climatic Research Unit at the University of East Anglia, United Kingdom
ECWMF	European Centre for Medium-Range Weather Forecast
ENSO	El Niño Southern Oscillation
ERA-40	ECWMF Reanalysis 40-year Product
IPCC	United Nations Intergovernmental Panel on Climate Change
ITCZ	Inter-tropical Convergence Zone
MOC	Meridional Overturning Circulation
NAO	North Atlantic Oscillation
NCAR	National Center for Atmospheric Research
NCEP	National Centers for Environmental Prediction
PDO	Pacific Decadal Oscillation
SAT	surface air temperature
SST	sea surface temperature
SSD	sunshine duration
THC	thermohaline circulation
TSI	Total Solar Irradiance
WPSD	wavelet power spectral density
WT	wavelet transform
XWT	cross-wavelet transform

Appendix B. The Morlet wavelet analysis

We have modified the original codes of Torrence and Compo (1998) and Grinsted et al. (2004) to calculate the wavelet transform of the Chinese surface air temperature, total solar irradiance, and Japanese sunshine duration time series. To analyze the evolution of periodicities in frequency–time domains, we use a wavelet analysis adopting Morlet wavelet as the mother function because it provides a higher resolution in periodicity/frequency and because that it being a complex function, it allows us to calculate the phase between two time series.

The Morlet wavelet, consists of a complex exponential function modulated by a Gaussian wavelet, is defined as

$$e^{i\omega_o t/s} e^{-t^2/(2s^2)}, \tag{A1}$$

where t is the time with $s=(frequency)^{-1}$ as the wavelet scale and ω_0 is a non-dimensional frequency. Here, $\omega_0=6$ to satisfy the admissibility condition (Farge, 1992). The wavelet power is calculated as

$$|W_n^X|^2, \tag{A2}$$

where W_n^X is the wavelet transform of a time series X and n is the time index (Torrence and Compo, 1998).

For calculating the wavelet transform, it is necessary that the time series have 2^n elements. If not, then it is filled with zeros and the cone of influence (COI) is the region of the wavelet spectrum outside which the edge effects become important (Torrence and Compo, 1998).

Wavelet Power Spectral Density (WPSD) is calculated for each parameter; the black thin lines in Figs. 2, 6, and 7 marks the 95% confidence interval or boundaries of COI. To determine significance levels of the global wavelet power spectrum, an appropriate background spectrum must be chosen (Torrence and Compo, 1998). For many phenomena, an appropriate background spectrum is either white noise (with a flat Fourier spectrum) or red noise (increasing power with decreasing frequency). We choose to establish our significance levels in the global wavelet spectra with a simple red noise model that represents an autoregressive linear Markov process (Gilman et al., 1963).

B.1. The cross wavelet analysis

For analysis of the covariance of two time series X_1 (input) and X_2 (output)—such as the Chinese Temperature, Japanese sunshine duration, and total solar irradiance time series—the cross-wavelet $W_k^{X_1X_2}(\psi)$ (XWT) was used which measures the common power between the input and output variables in the physical system, the synchronization in phase, frequency and/or amplitude.

The cross wavelet analysis of two time series X_1 (input) and X_2 (output) was introduced by Hudgins et al. (1993). Torrence and Compo (1998) defined the cross wavelet spectrum as

$$W_n^{X_1,X_2} = W_n^{X_1} W_n^{X_2*}, \tag{A3}$$

where ($*$) denotes complex conjugation, ($W_n^{X_1}$) and ($W_n^{X_2}$) are the wavelet transforms (WT) of the two time series X_1 and X_2. The cross wavelet energy is defined as $|W_n^{X_1,X_2}|$ while the complex argument is the local relative phase between X_1 and X_2 in time–frequency space. Torrence and Webster (1999) defined the cross-wavelet power as the square of the energy, $|W_n^{X_1,X_2}|^2$. The phase angle of W^{X_1,X_2} describes the phase relationship between the X_1 and X_2 series in time–frequency space. Statistical significance of the wavelet coherence is estimated using Monte Carlo methods with red noise to determine the 5% significance level (Torrence and Webster, 1999).

The arrows in the cross-wavelet spectra XWT show the phase between the two time series: arrows at 0° (pointing to the right) indicate that both time series are perfectly positively correlated (in phase) and arrows at 180° (pointing to the left) indicate that they are perfectly negatively correlated (180° out of phase). It is important to point out that these two cases imply a linear relationship between the considered phenomena. Non-horizontal arrows indicate an out of phase situation, meaning that the two studied phenomena have a more complex non-linear relationship.

B.2. The wavelet global spectra and global phase

On the left panels of Figs. 2, 6, and 7, the *global spectra* are shown. The global spectrum is an average of the power of each periodicity in both the wavelet and the cross spectra (*i.e.*, WT and XWT). It is usually used to view, *at a glance*, the global periodicities of either time series.

The significance level of the global wavelet spectra is indicated by the dashed curves; they refer to the power of the red noise level at the 95% confidence level that increases with decreasing frequency (Grinsted et al., 2004). The uncertainties of the periodicities of both global wavelet and cross-wavelet spectra are obtained at the half maximum of the full width peak.

The panels on the right of Figs. 2, 6, and 7 show the *global phase* information, which is an average phase angle of each periodicity in both the wavelet and the cross-wavelet spectra. It is usually used to notice, *at a glance*, the global phase of either time series. The bottom panel in Fig. 2 gives the instantaneous phase for the selected multidecadal oscillatory scale of 60-years, while the bottom panel in Figs. 6 and 7 gives relative phase for the 60-year-scale oscillation. Therefore, these panels provide information on the lead–lag relationship of the two time series.

References

Agnihotri, R., Dutta, K., 2003. Centennial scale variations in monsoonal rainfall (Indian, east equatorial and Chinese monsoons): manifestations of solar variability. Current Science 85, 459–463.

Akasofu, S.-I., 2010. On the recovery from the Little Ice Age. Natural Science 2, 1211–1224.

Anderson, T.L., Charlson, R.J., Schwartz, S.E., Knutti, R., Boucher, O., Rodhe, H., Heintzenberg, J., 2003. Climate forcing by aerosols—a hazy picture. Science 300, 1103–1104.

Baliunas, S.L., et al., 1995. Chromospheric variations in main-sequence stars. II. The Astrophysical Journal 438, 269–287.
Box, J.E., Yang, L., Bromwich, D.H., Bai, L.-S., 2009. Greenland ice sheet surface air temperature variability: 1840–2007. Journal of Climate 22, 4029–4049.
Bradley, R.S., Diaz, H.F., Jones, P.D., Kelly, P.M., 1987. Secular fluctuations of temperature over Northern Hemisphere land areas and mainland China since the mid-19th century. In: Ye, D., Fu, C., Chao, J., Yoshino, M. (Eds.), The Climate of China and Global Climate. China Ocean Press, Beijing, pp. 76–87.
Branstator, G., 2002. Circumglobal teleconnections, the jet stream waveguide, and the North Atlantic Oscillation. Journal of Climate 15, 1893–1910.
Bronninmann, S., 2009. Early twentieth-century warming. Nature Geoscience 2, 735–736.
Che, H.Z., Shi, G.Y., Zhang, X.Y., Arimoto, R., Zhao, J.Q., Xu, L., Wang, B., Chen, Z.H., 2005. Analysis of 40 years of solar radiation data from China, 1961–2000. Geophysical Research Letters 32, L06803. doi:10.1029/2004GL022322.
Chen, T.-C., 2002. A North Pacific short-wave train during the extreme phases of ENSO. Journal of Climate 15, 2359–2376.
Chung, C.E., Ramanathan, V., Carmichael, G., Kulkarni, S., Tang, Y., Adhikary, B., Leung, L.R., Qian, Y., 2010. Anthropogenic aerosol radiative forcing in Asia derived from regional models with atmospheric and aerosol data assimilation. Atmospheric Chemistry and Physics 10, 6007–6024.
Compo, G.P., et al., 2011. The twentieth century reanalysis project. Quarterly Journal of the Royal Meteorological Society 137, 1–28.
Compo, G.P., Whitaker, J.S., Sardeshmukh, P.D., 2006. Feasibility of a 100-year reanalysis using only surface pressure data. Bulletin of the American Meteorological Society 87, 175–190.
de Jager, C., Duhau, S., van Geel, B., 2010. Quantifying and specifying the solar influence on terrestrial surface temperature. Journal of Atmospheric and Solar-Terrestrial Physics 72, 926–937.
Diaz, H.F., Quayle, R.G., 1980. The climate of the United States since 1895: spatial and temporal changes. Monthly Weather Review 108, 249–266.
Ding, Q., Wang, B., 2005. Circumglobal teleconnection in the Northern Hemisphere summer. Journal of Climate 18, 3483–3505.
Ding, Q., Wang, B., Wallace, J.M., Branstator, G., 2011. Tropical-extratropical teleconnections in boreal summer: observed interannual variability. Journal of Climate 24, 1878–1896.
Ding, Y., Wang, Z., Sun, Y., 2007. Inter-decadal variation of the summer precipitation in East China and its association with decreasing Asian summer monsoon. Part I: observed evidences. International Journal of Climatology 28, 1139–1161.
Ding, Y.-J., Luo, B.-R., Feng, Y.-M., 1983. Peak years of various solar cycle. Chinese Astronomy and Astrophysics 7, 24–30.
Domingo, V., et al., 2009. Solar surface magnetism and irradiance on time scales from days to the 11-year cycle. Space Science Reviews 145, 337–380.
Dong, B., Sutton, R.T., Scaife, A.A., 2006. Multidecadal modulation of El Niño-Southern Oscillation (ENSO) variance by Atlantic Ocean sea surface temperatures. Geophysical Research Letters 33, L08705. doi:10.1029/2006GL025766.
Drinkwater, K.F., 2006. The regime shift of the 1920s and 1930s in the North Atlantic. Progress in Oceanography 68, 134–151.
Du, Z.L., 2006. A new solar activity parameter and the strength of 5-cycle periodicity. New Astronomy 12, 29–32.
Enomoto, T., Hoskins, B.J., Matsuda, Y., 2003. The formation mechanism of the Bonin high in August. Quarterly Journal of the Royal Meteorological Society 129, 157–178.
Farge, M., 1992. Wavelet transforms and their applications to turbulence. Annual Review of Fluid Mechanics 24, 395–457.
Feng, S., Hu, Q., 2008. How the North Atlantic Multidecadal Oscillation may have influenced the Indian summer monsoon during the past two millennia. Geophysical Research Letters 35, L01707. doi:10.1029/2007GL032484.
Frauenfeld, O.W., Knappenberger, P.C., Michaels, P.J., 2011. A reconstruction of annual Greenland ice melt extent, 1784–2009. Journal of Geophysical Research 116, D08104. doi:10.1029/2010JD014918.
Frauenfeld, O.W., Zhang, T., Serreze, M.C., 2005. Climate change and variability using European Centre for Medium-Range Weather Forecasts reanalysis (ERA-40) temperatures on the Tibetan Plateau. Journal of Geophysical Research 110, D02101. doi:10.1029/2004JD005230.
Frohlich, C., 2009. Evidence of a long-term trend in total solar irradiance. Astronomy and Astrophysics 501, L27–L30.
Fu, C., Diaz, H.F., Dong, D., Fletcher, J.O., 1999. Changes in atmospheric circulation over Northern Hemisphere oceans associated with the rapid warming of the 1920s. International Journal of Climatology 19, 581–606.
Ge, Q.-S., Zheng, J.-Y., Hao, Z.-X., Shao, X.-M., Wang, W.-C., 2010. Temperature variation through 2000 years in China: an uncertainty analysis of reconstruction and regional difference. Geophysical Research Letters 37, L03703. doi:10.1029/2009GL041281.
Giese, B.S., Compo, G.P., Slowey, N.C., Sardeshmukh, P.D., Carton, J.A., Ray, S., Whitaker, S., 2010. The 1918/19 El Niño. Bulletin of the American Meteorological Society 91, 177–183.
Gilman, D.L., Fugliste, E.J., Mitchell, J.R., 1963. On the power spectrum of "Red Noise". Journal of the Atmospheric Sciences 20, 182–184.
Gong, D., Ho, C.-H., 2002. Shift in the summer rainfall over the Yangtze River valley in the late 1970s. Geophysical Research Letters 29, 1436. doi:10.1029/2001GL014523.
Goswami, B.N., Madhusoodanan, M.S., Neema, C.P., Sengupta, D., 2006. A physical mechanism for North Atlantic SST influence on the Indian summer monsoon. Geophysical Research Letters 33, L02706. doi:10.1029/2006GL024803.
Grinsted, A., Moore, J., Jevrejeva, S., 2004. Application of the cross wavelet transform and wavelet coherence to geophysical time series. Nonlinear Processes in Geophysics 11, 561–566.
Guo, Q., Cai, J., Shao, X., Sha, W., 2004. Applicability evaluation of surface air temperature from several reanalysis datasets in China. Chinese Journal of Atmospheric Sciences 28, 206–215 (in Chinese with English abstract).
Hameed, S., Gong, G., 1994. Variation of spring climate in lower-middle Yangtse River Valley and its relation with solar-cycle length. Geophysical Research Letters 21, 2693–2696.
Helama, S., Fauria, M.M., Mielikainen, K., Timonen, M., Eronen, M., 2010. Sub-Milankovitch solar forcing of past climates: mid and late Holocene perspectives. Geological Society of America Bulletin 122, 1981–1988.
Heristchi, D., Mouradian, Z., 2009. The global rotation of solar activity structures. Astronomy and Astrophysics 497, 835–841.
Hinkelman, L.M., Stackhouse, P.W., Wielicki, B.A., Zhang, T., Wilson, S.R., 2009. Surface insolation trends from satellite and ground measurements: comparisons and challenges. Journal of Geophysical Research 114, D00D20. doi:10.1029/2008JD011004.
Holland, D.M., Thomas, R.H., de Young, B., Ribergaard, M.H., Lyberth, B., 2008. Acceleration of Jakobshavn Isbrae triggered by warm subsurface ocean waters. Nature Geoscience 1, 659–664.
Honda, M., Yamane, S., Nakamura, H., 2005. Impact of the Aleutian–Icelandic low seasaw on surface climate during the twentieth century. Journal of Climate 18, 2793–2802.
Hoyt, D.V., Schatten, K.H., 1993. A discussion of plausible solar irradiance variations, 1700–1992. Journal of Geophysical Research 98, 18895–18906.
Hsu, K.J., 1996. Could global warming be a blessing for mankind? Terrestrial, Atmospheric and Oceanic Sciences 7, 375–392.
Hudgins, L., Friehe, C.A., Mayer, M.E., 1993. Wavelet transforms and atmospheric turbulence. Physical Review Letters 71, 3279–3282.
Ikhsanov, R.N., Vitinskii, Yu.I., 1980. Differential rotation of the Sun of the Maunder Minimum. Soviet Physics Doklady 25, 664–666.
IPCC, 2007. In: Solomon, S., Qin, D., Manning, M., Chen, Z., Marquis, M., Averyt, K.B., Tignor, M., Miller, H.L. (Eds.), Climate Change 2007: Working Group I: The Physical Science Basis. Cambridge University Press, Cambridge, United Kingdom and New York, NY, USA.
Jones, P.D., Lister, D.H., Li, Q., 2008. Urbanization effects in large-scale temperature records, with an emphasis on China. Journal of Geophysical Research 113, D16122. doi:10.1029/2008JD009916.
Kaiser, D.P., Qian, Y., 2002. Decreasing trends in sunshine duration over China for 1954–1998: indication of increased haze pollution? Geophysical Research Letters 29, L2042. doi:10.1029/2002GL016057.
Kalnay, E., et al., 1996. The NCEP/NCAR 40-year reanalysis project. Bulletin of the American Meteorological Society 77, 437–471.
Kane, R.P., 2008. Prediction of solar cycle 24 based on the Gnevyshev-Ohl-Kopecky rule and the three-cycle periodicity scheme. Annales Geophysicae 26, 3329–3339.
Kauker, F., Koberle, C., Gerdes, R., Karcher, M., 2008. Modeling the 20th century Arctic ocean/sea ice system: reconstruction of surface forcing. Journal of Geophysical Research 113, C09027. doi:10.1029/2006JC004023.
Kiehl, J.T., 2007. Twentieth century climate model response and climate sensitivity. Geophysical Research Letters 34, L22710. doi:10.1029/2007GL031383.
Kirby, M.E., Mullins, H.T., Patterson, W.P., Burnett, A.W., 2002. Late glacial-Holocene atmospheric circulation and precipitation in the northeast United States inferred from modern calibrated stable oxygen and carbon isotopes. Geological Society of America Bulletin 114, 1326–1340.
Knudsen, M.F., Seidenkrantz, M.-S., Jacobsen, B.H., Kuijpers, A., 2010. Tracking the Atlantic Multidecadal Oscillation through the last 8,000 years. Nature Communications, 2. doi:10.1038/ncomms1186.
Knutti, R., 2008. Why are climate models reproducing the observed global surface warming so well? Geophysical Research Letters 35, L18704. doi:10.1029/2008GL034932.
Kollath, Z., Olah, K., 2009. Multiple and changing cycles of active stars. I. Methods of analysis and application to the solar cycles. Astronomy and Astrophysics 501, 695–702.
Kopp, G., Lean, J.L., 2011. A new, lower value of total solar irradiance: evidence and climate significance. Geophysical Research Letters 38, L01706. doi:10.1029/2010GL045777.
Kosaka, Y., Nakamura, H., Watanabe, M., Kimoto, M., 2009. Analysis on the dynamics of a wave-like teleconnection pattern along summertime Asian Jet based on a reanalysis dataset and climate model simulations. Journal of the Meteorological Society of Japan 87, 561–580.
Krivova, N.A., Solanki, S.K., Wenzler, T., 2009. ACRIM-gap and total solar irradiance revisited: is there a secular trend between 1986 and 1996? Geophysical Research Letters 36, L20101. doi:10.1029/2009GL040707.
Lau, K.-M., Lee, J.-Y., Kim, K.-M., Kang, I.-S., 2004. The North Pacific as a regulator of summertime climate over Eurasia and North America. Journal of Climate 17, 819–833.
Lau, K.-M., Weng, H., 2002. Recurrent teleconnection patterns linking summertime precipitation variability over East Asia and North America. Journal of the Meteorological Society of Japan 80, 1309–1324.
Lean, J., Rottman, G., Harder, J., Kopp, G., 2005. SORCE contributions to new understanding of global change and solar variability. Solar Physics 230, 27–53.
Lee, H.F., Zhang, D.D., 2010. Changes in climate and secular population cycles in China, 1000 CE to 1911. Climate Research 42, 235–246.
Li, J., Yu, R., Zhou, T., Wang, B., 2005. Why is there an early spring cooling shift downstream of the Tibetan Plateau? Journal of Climate 18, 4660–4668.

Li, L., Wang, B., Zhou, T., 2007. Contributions of natural and anthropogenic forcings to the summer cooling over eastern China: an AGCM study. Geophysical Research Letters 34, L18807. doi:10.1029/2007GL030541.
Li, Q., Li, W., Si, P., Gao, X., Dong, W., Jones, P., Huang, J., Cao, L., 2010. Assessment of surface air warming in northeast China, with emphasis on the impacts of urbanization. Theoretical and Applied Climatology 99, 469–478.
Li, S., Bates, G.T., 2007. Influence of Atlantic multidecadal oscillation on the winter climate of East China. Advances in Atmospheric Sciences 24, 126–135.
Li, S., Perlwitz, J., Quan, X., Hoerling, M.P., 2008. Modeling the influence of North Atlantic multidecadal warmth on the Indian summer rainfall. Geophysical Research Letters 35, L05804. doi:10.1029/2008GL032901.
Li, X., Li, W., Zhou, X., 1998. Analysis of the solar radiation variation of China in recent 30 years. Quarterly Journal of Applied Meteorology 19, 24–31 (in Chinese with English abstract).
Lin, H., 2009. Global extratropical response to diabatic heating variability of the Asian summer monsoon. Journal of the Atmospheric Sciences 66, 2697–2713.
Lin, X., Yu, S., Tang, G., 1995. Series of average air temperature over China for the last 100-year period. Scientia Atmospherica Sinica 19, 525–534 (in Chinese with English abstract).
Lindzen, R.S., Choi, Y.-S., 2011. On the observational determination of climate sensitivity and its implications. Asia-Pacific Journal of Atmospheric Sciences 47 (4), 377–390.
Liu, J., Wang, B., Ding, Q., Kuang, X., Soon, W., Zorita, E., 2009. Centennial variations of the global monsoon precipitation in the last millennium: results from ECHO-G model. Journal of Climate 22, 2356–2371.
Liu, S.C., Wang, C.-H., Shiu, C.-J., Chang, H.-W., Hsiao, C.-K., Liaw, S.-H., 2002. Reduction in sunshine duration over Taiwan: causes and implications. Terrestrial, Atmospheric and Oceanic Sciences 13, 523–545.
Lu, R., Dong, B., Ding, H., 2006. Impact of Atlantic multidecadal oscillation on the Asian summer monsoon. Geophysical Research Letters 33, L24701. doi:10.1029/2006GL027655.
Ma, L., Zhang, T., Li, Q., Frauenfeld, O.W., Qin, D., 2008. Evaluation of ERA-40, NCEP-1, and NCEP-2 reanalysis air temperatures with ground-based measurements in China. Journal of Geophysical Research 113, D15115. doi:10.1029/2007JD009549.
Meehl, G.A., Arblaster, J.M., Branstator, G., van Loon, H., 2008. A coupled air-sea response mechanism to solar forcing in the Pacific region. Journal of Climate 21, 2883–2897.
Minobe, S., 1997. A 50–70 year oscillation over the North Pacific and North America. Geophysical Research Letters 24, 683–686.
Mitchell, T.D., Hulme, M., New, M., 2002. Climate data for political areas. Area 34, 109–112.
Miyahara, H., Yokoyama, Y., Masuda, K., 2008. Possible link between multi-decadal climate cycles and periodic reversals of solar magnetic polarity. Earth and Planetary Science Letters 272, 290–295.
Myhre, G., 2009. Consistency between satellite-derived and modeled estimates of the direct aerosol effect. Science 325, 187–190.
Nitta, T., 1987. Convective activities in the tropical Western Pacific and their impact on the Northern Hemisphere summer circulation. Journal of the Meteorological Society of Japan 65, 373–390.
Norris, J.R., Wild, M., 2009. Trends in aerosol radiative effects over China and Japan inferred from observed cloud cover, solar "dimming", and solar "brightening". Journal of Geophysical Research 114, D00D15. doi:10.1029/2008JD011378.
Norris, J.R., Zhang, Y., Wallace, J.M., 1998. Role of low clouds in summertime atmosphere–ocean interactions over the North Pacific. Journal of Climate 11, 2482–2490.
Ohmura, A., 2006. Observed long-term variations of solar irradiance at the Earth's surface. Space Science Reviews 125, 111–128.
Ohvril, H., et al., 2009. Global dimming and brightening versus atmospheric column transparency, Europe, 1906–2007. Journal of Geophysical Research 114. D00D12. doi:10.1029/2008JD010644.
Pavlakis, K.G., Hatzianastassiou, N., Matsoukas, C., Fotiadi, A., Vardavas, I., 2008. ENSO surface shortwave radiation forcing over the tropical Pacific. Atmospheric Chemistry and Physics 8, 5565–5577.
Pielke, R., et al., 2009. Climate change: the need to consider human forcings besides greenhouse gases. Eos, Transactions of the American Geophysical Union 90, p. 413.
Portman, D.A., 1993. Identifying and correcting urban bias in regional time series: surface temperature in China's northern plains. Journal of Climate 6, 2298–2308.
Powell, A.M., Xu, J., 2011. A new assessment of the mid-1970s abrupt atmospheric temperature change in the NCEP/NCAR reanalysis and associated solar forcing implications. Theoretical and Applied Climatology 104, 443–458.
Powell, A.M., Xu, J., Comparisons of temperature response to solar forcing in the pre- and post periods of satellite data assimilation. International. Journal of Climatology, in press. doi:10.1002/joc.2239.
Qian, C., Wu, Z., Fu, C., Zhou, T., 2010. On multi-timescale variability of temperature in China in modulated annual cycle reference frame. Advances in Atmospheric Sciences 27, 1169–1182.
Qian, Y., Wang, W., Leung, L.R., Kaiser, D.P., 2007. Variability of solar radiation under cloud-free skies in China: the role of aerosols. Geophysical Research Letters 34, L12804. doi:10.1029/2006GL028800.
Rajeevan, M., Sridhar, L., 2008. Inter-annual relationship between Atlantic sea surface temperature anomalies and Indian summer monsoon. Geophysical Research Letters 35, L21704. doi:10.1029/2008GL036025.
Ren, G., Zhou, Y., Chu, Z., Zhou, J., Zhang, A., Guo, J., Liu, X., 2008. Urbanization effects on observed surface air temperature trends in northern China. Journal of Climate 21, 1333–1348.
Rogers, J.C., 1985. Atmospheric circulation changes associated with the warming over the Northern North Atlantic in the 1920s. Journal of Climate and Applied Meteorology 24, 1303–1310.
Ruckstuhl, C., Norris, J.R., 2009. How do aerosol histories affect solar "dimming" and "brightening" over Europe?: IPCC-AR4 models versus observations. Journal of Geophysical Research 114, D00D04. doi:10.1029/2008JD011066.
Sato, N., Takahashi, M., 2006. Dynamical processes related to the appearance of quasi-stationary waves on the subtropical jet in the midsummer Northern Hemisphere. Journal of Climate 19, 1531–1544.
Scafetta, N., Willson, R., 2009. ACRIM-gap and TSI trend issue resolved using a surface magnetic flux TSI proxy model. Geophysical Research Letters 36, L05701. doi:10.1029/2008GL036307.
Schlesinger, M.E., Ramankutty, N., 1994. An oscillation in the global climate system of period 65–70 years. Nature 367, 723–726.
Schneider, D.P., Steig, E.J., 2008. Ice cores record significant 1940s Antarctic warmth related to tropical climate variability. Proceedings of the U.S. National Academy of Sciences 105, 12154–12158.
Screen, J.A., Simmonds, I., 2011. Erroneous Arctic temperature trends in the ERA-40 reanalysis: a closer look. Journal of Climate 24, 2620–2627.
Selten, F.M., Branstator, G.W., Dijkstra, H.A., Kliphuis, M., 2004. Tropical origins for recent and future Northern Hemisphere climate change. Geophysical Research Letters 31, L21205. doi:10.1029/2004GL020739.
Shapiro, A.I., Schmutz, W., Rozanov, E., Schoell, M., Haberreiter, M., Shapiro, A.V., Nyeki, S., 2011. A new approach to the long-term reconstruction of the solar irradiance leads to a large historical solar forcing. Astronomy and Astrophysics 529, A67.
Shi, G.-Y., Hayasaka, T., Ohmura, A., Chen, Z.-H., Wang, B., Zhao, J.-Q., Che, H.-Z., Xu, L., 2008. Data quality assessment and the long-term trend of ground solar radiation in China. Journal of Applied Meteorology and Climatology 47, 1006–1016.
Soon, W.W.-H., 2005. Variable solar irradiance as a plausible agent for multidecadal variations in the Arctic-wide surface air temperature record of the past 130 years. Geophysical Research Letters 32, L16712. doi:10.1029/2005GL023429.
Soon, W., 2007. Implications of the secondary role of carbon dioxide and methane forcing in climate change: past, present, and future. Physical Geography 28, 97–125.
Soon, W., 2009. Solar Arctic-mediated climate variation on multidecadal to centennial timescales: empirical evidence, mechanistic explanation, and testable consequences. Physical Geography 30, 144–184.
Soon, W., Baliunas, S., Idso, C., Idso, S., Legates, D.R., 2003. Reconstructing climatic and environmental changes of the past 1000 years: a reappraisal. Energy and Environment 14, 233–296.
Soon, W., Legates, D.R., 2010. Avoiding carbon myopia: three considerations for policymakers concerning manmade carbon dioxide. Ecology Law Currents 37, 1–9.
Stanhill, G., Cohen, S., 2001. Global dimming: a review of the evidence for a widespread and significant reduction in global radiation with discussion of its probable causes and possible agricultural consequences. Agricultural and Forest Meteorology 107, 255–278.
Stanhill, G., Cohen, S., 2005. Solar radiation changes in the United States during the twentieth century: evidence from sunshine duration measurements. Journal of Climate 18, 1503–1512.
Stanhill, G., Cohen, S., 2008. Solar radiation changes in Japan during the 20th century: evidence from sunshine duration measurements. Journal of the Meteorological Society of Japan 86, 57–67.
Sun, J., Wang, H., Yuan, W., 2008. Decadal variations of the relationship between the summer North Atlantic Oscillation and middle East Asian air temperature. Journal of Geophysical Research 113, D15107. doi:10.1029/2007JD009626.
Tang, G., Ding, Y., Wang, S.W., Ren, G., Liu, H., Zhang, L., 2009. Comparative analysis of the time series of surface air temperature over China for the last 100 years. Advances in Climate Change Research 5, 71–78 (in Chinese with English abstract).
Timmermann, A., et al., 2007. The influence of a weakening of the Atlantic meridional overturning circulation on ENSO. Journal of Climate 20, 4899–4919.
Torrence, C., Compo, G., 1998. A practical guide to wavelet analysis. Bulletin of the American Meteorological Society 79, 61–78.
Torrence, C., Webster, P., 1999. Interdecadal changes in ENSO–Monsoon system. Journal of Climate 12, 2679–2690.
Usoskin, I., Mironova, I.A., Korte, M., Kovaltsov, G.A., 2010. Regional millennial trend in the cosmic ray induced ionization of the troposphere. Journal of Atmospheric and Solar-Terrestrial Physics 72, 19–25.
van Loon, H., Meehl, G.A., Arblaster, J.M., 2004. A decadal solar effect in the tropics in July–August. Journal of Atmospheric and Solar-Terrestrial Physics 66, 1767–1778.
Wakabayashi, S., Kawamura, R., 2004. Extraction of major teleconnection patterns possibly associated with the anomalous summer climate in Japan. Journal of the Meteorological Society of Japan 82, 1577–1588.
Wang, B., Bao, Q., Hoskins, B., Wu, G., Liu, Y., 2008. Tibetan Plateau warming and precipitation changes in East Asia. Geophysical Research Letters 35, L14702. doi:10.1029/2008GL034330.
Wang, K., Dickinson, R.E., Liang, S., 2007. Clear sky visibility has decreased over land globally from 1973 to 2007. Science 323, 1468–1470.
Wang, S.W., 1990. Reconstruction of the temperature series of northern China back to 1380 AD. Science in China B 5, 553–560 (in Chinese).
Wang, S., Gong, D., 2000. Enhancement of the warming trend in China. Geophysical Research Letters 27, 2581–2584.

Wang, S., Gong, D., Zhu, J., 2001. Twentieth-century climatic warming in China in the context of the Holocene. Holocene 11, 313–321.
Wang, S., Luo, Y., Zhao, Z., Dong, W., Yang, B., 2006. Debating about the climate warming. Progress in Natural Science 16, 1–6.
Wang, S.W., Zhu, J., Chai, J., 2004. Interdecadal variability of temperature and precipitation in China since 1880. Advances in Atmospheric Sciences 21, 307–313.
Wang, X., Zhang, Q.-B., 2011. Evidence of solar signals in tree rings of Smith fir from Sygera Mountain in southeast Tibet. Journal of Atmospheric and Solar-Terrestrial Physics 73, 1959–1966.
Wang, Y., Li, S., Luo, D., 2009. Seasonal response of Asian monsoonal climate to the Atlantic multidecadal oscillation. Journal of Geophysical Research 114, D02112. doi:10.1029/2008JD010929.
Wang, Y.M., Lean, J.L., Sheeley, N.R., 2005. Modeling the sun's magnetic field and irradiance since 1713. The Astrophysical Journal 625, 522–538.
Watanabe, M., 2004. Asian jet waveguide and a downstream extension of the North Atlantic Oscillation. Journal of Climate 17, 4674–4691.
Wen, X.-Y., Wang, S.-W., Zhu, J.-H., Viner, D., 2006. An overview of China climate change over the 20th century using UK UEA/CRU high resolution grid data. Chinese Journal of Atmospheric Sciences 30, 894–904 (in Chinese with English abstract).
Weng, H., 2005. The influence of the 11 yr solar cycle on the interannual–centennial climate variability. Journal of Atmospheric and Solar-Terrestrial Physics 67, 793–805.
Wenzler, T., Solanki, S.K., Krivova, N.A., 2009. Reconstructed and measured total solar irradiance: is there a secular trend between 1978 and 2003? Geophysical Research Letters 36, L11102. doi:10.1029/2009GL037519.
Wild, M., Trussel, B., Ohmura, A., Long, C.N., Konig-Langlo, G., Dutton, E.G., Tsvetkov, A., 2009. Global dimming and brightening: an update beyond 2000. Journal of Geophysical Research 114, D00D13. doi:10.1029/2008JD011382.
Wood, K.R., Overland, J.E., 2010. Early 20th century Arctic warming in retrospect. International Journal of Climatology 30, 1269–1279. doi:10.1002/joc.1973.
Wood, K.R., Overland, J.E., Jonsson, T., Smoliak, B.V., 2010. Air temperature variations on the Atlantic–Arctic boundary since 1802. Geophysical Research Letters 37, L17708. doi:10.1029/2010GL044176.
Wu, G., Liu, Y., Wang, T., Wan, R., Liu, X., Li, W., Wang, Z., Zhang, Q., Duan, A., Liang, X., 2007. The influence of mechanical and thermal forcing by the Tibetan Plateau on Asian climate. Journal of Hydro Meteorology 8, 770–789.
Wu, S., Liu, Z., Zhang, R., Delworth, T.L., 2011. On the observed relationship between the Pacific Decadal Oscillation and the Atlantic Multi-decadal Oscillation. Journal of Oceanography 67, 27–35.
Xia, X.A., Wang, P.C., Chen, H.B., Liang, F., 2006. Analysis of downwelling surface solar radiation in China from National Centers for Environmental Prediction reanalysis, satellite estimates, and surface observations. Journal of Geophysical Research 111, D09103. doi:10.1029/2005JD006405.
Xu, Z.-T., 1990. Solar observations in ancient China and solar variability. Philosophical Transactions of the Royal Society A 330, 513–515.
Yadav, R.K., 2009. Role of equatorial central Pacific and northwest of North Atlantic 2-metre surface temperatures in modulating Indian summer monsoon variability. Climate Dynamics 32, 549–563.
Yang, B., Braeuning, A., Johnson, K.R., Shi, Y., 2002. General characteristics of temperature variation in China during the last two millennia. Geophysical Research Letters 29, L01324. doi:10.1029/2001GL014485.
Yang, J., Liu, Q., Liu, Z., Wu, L., Huang, F., 2009. Basin mode of Indian Ocean sea surface temperature and Northern Hemisphere circumglobal teleconnection. Geophysical Research Letters 36, L19705. doi:10.1029/2009GL039559.
Yang, S.L., Milliman, J.D., Li, P., Xu, K., 2011. 50,000 dams later: erosion of the Yangtze River and its delta. Global and Planetary Change 75, 14–20.
Yoshimura, H., 1979. The solar-cycle period-amplitude relation as evidence of hysteresis of the solar-cycle nonlinear magnetic oscillation and the long-term (55 year) cyclic modulation. The Astrophysical Journal 227, 1047–1058.
You, Q., Kang, S., Pepin, N., Flugel, W.-A., Yan, Y., Behrawan, H., Huang, J., 2010. Relationship between temperature trend magnitude, elevation and mean temperature in the Tibetan Plateau from homogenized surface stations and reanalysis data. Global and Planetary Change 71, 124–133.
Zhang, J., Dong, W., Wu, L., Wei, J., Chen, P., Lee, D.-K., 2005. Impact of land use changes on surface warming in China. Advances in Atmospheric Sciences 22, 343–348.
Zhang, R., Delworth, T.L., 2007. Impact of the Atlantic multidecadal oscillation on North Pacific climate variability. Geophysical Research Letters 34, L23708. doi:10.1029/2007GL031601.
Zhang, Q., Soon, W.H., Baliunas, S.L., Lockwood, G.W., Skiff, B.A., Radick, R.R., 1994. A method of determining possible brightness variations of the Sun in past centuries from observations of solar-type stars. The Astrophysical Journal Letters 427, L111–L114.
Zhang, Y., Norris, J.R., Wallace, J.M., 1998. Seasonality of large-scale atmosphere–ocean interaction over the North Pacific. Journal of Climate 11, 2473–2481.
Zhao, T., Fu, C., 2009. Applicability evaluation of surface air temperature from several reanalysis datasets in China. Plateau Meteorology 28, 594–606 (in Chinese with English abstract).
Zhao, Z., Ding, Y., Luo, Y., Wang, S., 2005. Recent studies on attributions of climate change in China. Acta Meteorologica Sinica 19, 389–400.
Zhou, L., Dickinson, R.E., Tian, Y., Fang, J., Li, Q., Kaufmann, R.F., Tucker, C.J., Myneni, R.B., 2004. Evidence for a significant urbanization effect on climate in China. Proceedings of the U.S. National Academy of Sciences 101, 9540–9544.
Zhou, T., Gong, D., Li, J., Li, B., 2009a. Detecting and understanding the multi-decadal variability of the East Asian Summer Monsoon-Recent progress and state of affairs. Meteorologische Zeitschrift 18, 455–467.
Zhou, T., et al., 2009b. Why the western Pacific subtropical high has extended westward since the late 1970s. Journal of Climate 22, 2199–2215.
Zhou, T., Yu, R., 2006. Twentieth-century surface air temperature over China and the globe simulated by coupled climate models. Journal of Climate 19, 5843–5858.
Zhou, T., Zou, L., 2010. Understanding the predictability of East Asian summer monsoon from the reproduction of land–sea thermal contrast change in AMIP-type simulation. Journal of Climate 23, 6009–6026.
Zhu, K., 1973. A preliminary study on the climatic fluctuations during the last 5000 years in China. Scientia Sinica 16, 226–256.
Zhu, J., Wang, S., 2002. 80 yr oscillation of summer rainfall over North China and East Asian Summer Monsoon. Geophysical Research Letters 29, L01672. doi:10.1029/2001GL013997.